

# Two-Gradient Convection in a Vertical Slot with Maxwell–Cattaneo Heat Conduction

N. C. Papanicolaou\*, C. I. Christov† and P. M. Jordan\*\*‡

\**Department of Computer Science, University of Nicosia, P.O. Box 24005, 1700 Nicosia, Cyprus*

†*Department of Mathematics, University of Louisiana at Lafayette, LA 70504–1010, USA*

\*\**Entropy Reversal Consultants (L.L.C.), P. O. Box 691, Abita Springs, LA 70420, USA*

‡*Code 7181, Naval Research Lab., Stennis Space Ctr., MS 39529, USA*

**Abstract.** We study the effect of the Maxwell–Cattaneo law of heat conduction (MCHC) on the 1D flow in a vertical slot subject to both vertical and horizontal temperature gradients. The gravitational acceleration is allowed to oscillate, which provides an opportunity to investigate the quantitative contribution of thermal inertia as epitomized by MCHC. The addition of the time derivative in MCHC increases the order of the system. We use a spectral expansion with Rayleigh’s beam functions as the basis set, which is especially suited to fourth order boundary value problems (BVP). We show that the time derivative (relaxation of the thermal flux) has a dissipative nature and leads to the appearance of purely real negative eigenvalues. Yet it also increases the absolute value of the imaginary part and decreases the absolute value of the real part of the complex eigenvalues. Thus, the system has a somewhat more oscillatory behavior than the one based on Fourier’s heat conduction law (FHC).

**Keywords:** Maxwell–Cattaneo law of heat conduction, two-gradient convection, g-jitter, beam functions.

**PACS:** 02.70.Hm, 44.10. i, 44.25.+f, 47.20.Bp, 47.11.Kb

## INTRODUCTION

One of the main shortcomings of Fourier’s law of heat conduction (FHC) is that it leads to a parabolic equation for the temperature field. This means that any initial disturbance is felt instantly, but unequally, throughout the entire medium in question. This behavior is said to contradict the principle of causality; and is known as the ‘paradox of heat conduction’ (PHC). To remedy this unrealistic feature, various modifications of Fourier’s law have been proposed over the years, not all of which have been successful (see, e.g., [1]). Of the formulations that have proven physically acceptable, the best known is the Maxwell–Cattaneo law of heat conduction (MCHC) [2, 3, 4, 5, 6]

$$(1 + \tau_0 \partial_t) \mathbf{q} = -\kappa \nabla T, \quad (1)$$

where  $\partial_t$  stands for the partial time derivative and  $\mathbf{q}$  denotes the heat flux vector, which predicts the existence of thermal waves. Here,  $\kappa (> 0)$  denotes the thermal conductivity, and the thermal relaxation characteristic time  $\tau_0 (> 0)$  represents the time lag required to establish steady heat conduction in a volume element, once a temperature gradient has been imposed across it [4].

While successful in many ways [2, 3, 4, 5], Eq. (1) does suffer one notable drawback: it is not invariant upon changing to a moving frame. This issue was discussed in [7],

where it was argued that the simple time derivative had to be replaced by an invariant rate, specifically, the convective (or material) derivative. Subsequently, in [8], a more general invariant time derivative (or ‘objective rate’) was used, namely, the Oldroyd upper-convected derivative, which is invariant in a generally accelerating and deforming coordinate system connected with the medium in which the heat propagates. The frame indifferent MCHC reads (see [8])

$$\tau_0 \left[ \frac{\partial \mathbf{q}}{\partial t} + \mathbf{v} \cdot \nabla \mathbf{q} - \mathbf{q} \cdot \nabla \mathbf{v} + (\nabla \cdot \mathbf{v}) \mathbf{q} \right] + \mathbf{q} = -\kappa \nabla T. \quad (2)$$

An important feature of the Frame Indifferent Maxwell–Cattaneo Law (FIMC) is that it gives a single equation for the heat conduction

$$\tau_0 [T_{tt} + 2\mathbf{v} \cdot \nabla T_t + \mathbf{v}_t \cdot \nabla T + (T_t + \mathbf{v} \cdot \nabla T)(\nabla \cdot \mathbf{v}) + \mathbf{v} \cdot \nabla(\mathbf{v} \cdot \nabla T)] + T_t + \mathbf{v} \cdot \nabla T = \nabla \cdot (\lambda \nabla T), \quad \lambda = \frac{\kappa}{\rho c_p}, \quad (3)$$

where  $\lambda$  is called the ‘coefficient of heat diffusivity.’

To better understand the consequences of this material invariant (or frame indifferent) formulation, in this work, we study the flow of an incompressible Newtonian fluid in a vertical slot subject to both a vertical and a horizontal temperature gradient [9]. It should be noted that this flow was thoroughly investigated in [10, 11, 12, 13] under FHC and with time dependent gravity (the so-called  $g$ -jitter flow). To highlight the role of the different terms in the objective rate, we at first investigate the limiting case of constant gravity using a truncated Galerkin expansions. We then proceed to a numerical investigation of the stability of MCHC-based  $g$ -jitter flow.

## CONVECTION IN A VERTICAL SLOT

Following [11, 13], we consider natural convection in a vertical fluid with differentially heated lateral surfaces. The  $x$ -axis is across the slot and  $y$  is taken as the vertical coordinate. The fluid fills the strip between the planes  $x = -h$  and  $x = h$  (see Figure 1).

In this work,  $\rho$  is the mass density,  $\nu$  is the kinematic viscosity, and  $\lambda$  is the above defined thermal diffusivity. Additionally,  $u, v$  are the  $x, y$ -components of the velocity;  $T$  is the temperature; and  $T_-$  and  $T_+$  are the temperatures of the left and right walls at position  $y = 0$ . Furthermore,  $\Delta_T$  is the vertical temperature gradient and the horizontal temperature differential is  $\beta = (T_+ - T_-)/h$ . We assume  $T_+ > T_-$ , without loss of generality, and we define the reference temperature as  $T_R = (T_+ + T_-)/2$ .

It is convenient to introduce the dynamic dimensionless variables as follows:

$$t = \hat{t} \frac{h}{U}, \quad x = h\hat{x}, \quad y = h\hat{y}, \quad u = \hat{u}U, \quad v = \hat{v}U, \quad (4)$$

where the characteristic velocity of the convective motion is  $U = \nu/h$ , and the dimensionless temperature can be defined as  $T - T_R = (\theta + \frac{1}{2}\frac{x}{h} + \delta\frac{y}{h})h\beta$ , where  $\delta = \Delta_T/\beta$

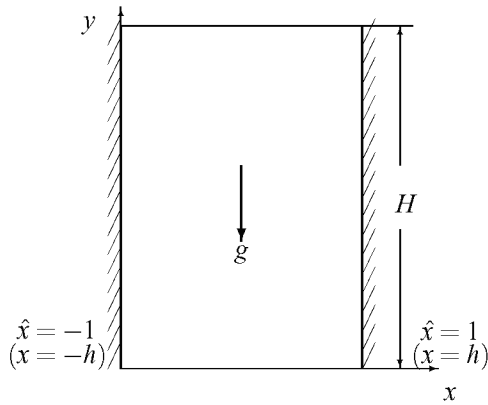


**FIGURE 1.** Flow geometry

is the relative vertical gradient of the temperature. And along with  $\delta$ , we also introduce the dimensionless complexes

$$\tau_C = \frac{\tau_0 \nu}{h^2}, \quad \text{Ra} = \frac{g \alpha \beta h^4}{\nu \lambda}, \quad \text{Pr} = \frac{h U}{\lambda} \equiv \frac{\nu}{\lambda}, \quad (5)$$

which are termed the Cattaneo, Rayleigh, and Prandtl numbers, respectively.

It can be shown that in terms of the stream function (see [11, 13] and the literature cited therein), the 1D equation of motion reads

$$\frac{\partial^3 \Psi}{\partial x^2 \partial t} = -\text{Ra} \left[ \frac{\partial \Theta(x, t)}{\partial x} + \frac{1}{2} \right] [1 + \varepsilon \cos(\omega t)] + \frac{\partial^4 \Psi}{\partial x^4}, \quad (6)$$

where  $\varepsilon$  and  $\omega$  are the dimensionless amplitude and frequency of the gravity modulations. (For the case of steady gravity,  $\varepsilon = 0$ .) The equation for the temperature field is based on [8, 14], and in terms of the stream function reads

$$\tau_C \frac{\partial^2 \Theta}{\partial t^2} - \delta \tau_C \frac{\partial^2 \Psi}{\partial x \partial t} + \frac{\partial \Theta}{\partial t} - \delta \frac{\partial \Psi}{\partial x} = \frac{1}{\text{Pr}} \frac{\partial^2 \Theta}{\partial x^2}, \quad (7)$$

which naturally encompasses FHC by simply setting  $\tau_C = 0$ . In terms of the above dimensionless quantities, the boundary conditions are given by

$$\Psi(\pm 1, t) = \partial_x \Psi|_{x=\pm 1} = 0, \quad \Theta(\pm 1, t) = 0, \quad (8)$$

which completes the formulation of the initial-boundary value problem under consideration.

## TRUNCATED GALERKIN EXPANSIONS

Our first task is to investigate system (6), (7), (8) for the case of steady gravity ( $\varepsilon = 0$  in (6)) using a truncated Galerkin expansion. In doing so, we compare the results obtained for FHC ( $\tau_c = 0$ ) with MCHC for  $\tau_c = 0.01$ .

Our basis functions are Lord Rayleigh's beam functions [15] and the trigonometric functions. The suitability of these two sets of functions, for problem of this kind, has been well-established (see [13] and the literature cited therein). All relevant formulas for the expansion of the various derivatives of the beam-functions into series with respect to the system, as well as the cross-expansion formulas, are given in the Appendix for the convenience of the reader.

We expand the unknown functions  $\Psi$  and  $\Theta$  as follows:

$$\Psi(x, t) = \sum_{i=1}^N p_i(t) c_i(x), \quad \Theta(x, t) = \sum_{i=1}^N d_i(t) \sin(i\pi x). \quad (9)$$

where, due to symmetry, we need only use even beam functions for  $\Psi$  and odd trigonometric functions for  $\Theta$ . Let us now substitute these expansions into Eqs. (6), (7) and employ the necessary expansion formulas (see the Appendix) to obtain the dynamical system

$$\sum_{j=1}^N \beta_{ij} \dot{p}_i = -\text{Ra} \left( \sum_{i=1}^N (i\pi) \chi_{ij} \dot{d}_i + \frac{\sqrt{2} \tanh \kappa_j}{\kappa_j} \right) + \kappa_j^4 p_j, \quad (10)$$

$$\tau_c \left[ \ddot{d}_j - \delta \sum_{i=1}^N b_{ij} \dot{p}_i \right] + \dot{d}_j - \delta \sum_{i=1}^N b_{ij} p_i = -\frac{j^2 \pi^2}{\text{Pr}} d_j \quad (11)$$

where  $b_{ij} = \sum_{k=1}^N a_{ik} \hat{\sigma}_{kj}$  ( $j = 1, 2, \dots, N$ ) and a superposed dot denotes the time derivative.

Next, we re-write Eqs. (10), (11) in the form  $\dot{\mathbf{y}} = \mathbf{A}\mathbf{y} + \mathbf{g}$  with the aid of the vectors

$$\{y_i\}_{i=1}^N := \{p_i\}_{i=1}^N, \quad \{y_i\}_{i=N+1}^{2N} := \{d_i\}_{i=1}^N, \quad \{y_i\}_{i=2N+1}^{3N} := \{e_i\}_{i=1}^N := \{\dot{d}_i\}_{i=1}^N. \quad (12)$$

Respectively,  $\mathbf{A}$  is the block matrix

$$\mathbf{A} = \begin{pmatrix} (C^T)^{-1} \mathbf{K} & -\text{Ra} (C^T)^{-1} \mathbf{X}^T & 0 \\ 0 & 0 & \mathbf{I} \\ \delta \mathbf{B}^T (C^T)^{-1} \mathbf{K} + \frac{\delta}{\tau_c} \mathbf{B}^T & -\delta \mathbf{B}^T \text{Ra} (C^T)^{-1} \mathbf{X}^T - \frac{1}{\tau_c} \frac{1}{\text{Pr}} \mathbf{\Pi}_2 & -\frac{1}{\tau_c} \mathbf{I} \end{pmatrix}. \quad (13)$$

Here,  $\mathbf{I} = [\delta_{ij}]$  is the  $N \times N$  unit matrix, where  $\delta_{ij}$  is Kronecker's delta,  $0$  is the zero matrix,  $\mathbf{C} = [\beta_{ij}]$ ,  $\mathbf{K} = [\kappa_i^4 \delta_{ij}]$ ,  $\mathbf{X} = [j\pi \chi_{ij}]$ ,  $\mathbf{h} = [h_j]$  (see Eq. (23)),  $\mathbf{B} = [b_{ij}]$ , and  $\mathbf{\Pi}_2 = [\delta_{ij} j^2 \pi^2]$ .

The block array  $\mathbf{g}$  is defined by

$$\{g_j\}_1^N := -\frac{\text{Ra}}{2} (C^T)^{-1} \mathbf{h}, \quad \{g_j\}_{N+1}^{2N} := \mathbf{0}, \quad \{g_j\}_{2N+1}^{3N} := -\frac{\text{Ra}}{2} \delta \mathbf{B}^T (C^T)^{-1} \mathbf{h} \quad (14)$$

For the case  $\tau_C > 0$ , if we take  $N$  terms in expansions (9), we obtain a  $3N \times 3N$  system, and  $A$  has  $3N$  eigenvalues. However, for the FHC case ( $\tau_C = 0$ ) we have a  $2N \times 2N$  system and

$$A = \begin{pmatrix} (C^T)^{-1}K & -Ra(C^T)^{-1}X^T \\ \delta B^T & -\delta B^T Ra(C^T)^{-1}X^T - \frac{1}{Pr}\Pi_2 \end{pmatrix}, \quad (15)$$

which obviously has  $2N$  eigenvalues.

Below, in Table 1, we present the eigenvalues for  $N = 1, 3, 7$ , which were obtained using Mathematica ©.

These results were obtained for the parameter set  $Pr = 0.73$ ,  $Ra = 10^5$ ,  $\delta = 0.15$ , and

**TABLE 1.** Eigenvalues for different number of terms

MCHC	FHC
Single-term expansion	
$-7.59763 \pm 125.053583 i$	$-11.84595 \pm 117.87638 i$
-94.97664	-
Three-terms expansion	
$-7.49831 \pm 125.63745 i$	$-11.73329 \pm 122.13555 i$
$-27.01868 \pm 136.43189 i$	$-47.10102 \pm 120.61122 i$
$-47.73177 \pm 150.61911 i$	$-107.07922 \pm 112.15192 i$
-86.43689	-
-96.61529	-
-94.99729	-
Seven-terms expansion	
$-7.68743 \pm 125.54751 i$	$-11.69540 \pm 122.42489 i$
$-28.51207 \pm 136.40804 i$	$-46.78391 \pm 122.10846 i$
$-46.40667 \pm 135.91944 i$	$-105.28525 \pm 121.01446 i$
$-48.75617 \pm 159.66046 i$	$-187.27435 \pm 118.25278 i$
$-50.01591 \pm 252.49780 i$	$-292.96854 \pm 112.42683 i$
$-50.05936 \pm 214.95036 i$	$-423.09242 \pm 101.14970 i$
$-50.36049 \pm 177.70430 i$	$-583.49800 \pm 76.68097 i$
-86.41509	-
-94.90617	-
-95.03107	-
-156.83333	-
-247.62508	-
359.15629	-
-504.83167	-

$\tau_C = 0.01$  was taken for the MCHC case. Clearly, the eigenvalues converge with the number of terms taken, because those with lower numbers do not change much when adding more terms in the expansion; in fact, even the one-term expansion is qualitatively very good in predicting the behavior of the system: stable or unstable. Eigenvalues with positive real parts mean exponential growth of the coefficients  $p_i(t)$ ,  $d_i(t)$ , and hence they imply instability, whereas  $\Re(\mu_i) < 0$  pertain to decaying oscillations.

Thus, for this parameter set, and for steady gravity, both the MCHC and FHC cases are stable. As expected, this behavior is observed also for other Rayleigh numbers in the

interval  $Ra < 100000$ . The results presented in Table 1 also show that adding a relaxation term in the heat conduction law has the following two, somewhat opposing, effects.

- (i) The oscillatory modes decay slower than the FHC case. In addition, the frequencies are slightly higher. This means that the oscillatory transients will decay in a longer time, making the system less damped as far as oscillations are concerned. This might have the effect of lowering the threshold of instability in the unsteady case, and we will investigate this in the next section.
- (ii) Negative real eigenvalues appear for the MCHC system. This signals the appearance of non-oscillatory, strongly damped transients, which are not present under FHC. This means that when in a subcritical stable regime, the MCHC system is more damped overall. The reason is that the energy will decay faster, because a sizable portion of it is redistributed into the non-oscillatory transients, which decay rapidly.

The opposing effects of the MCHC model compel us to treat a genuinely unsteady case. The natural platform for this investigation is the flow with unsteady gravity, i.e., the  $g$ -jitter flow.

## THE UNSTEADY GRAVITY CASE

In order to treat the  $g$ -jitter flow, we use the following numerical scheme

$$\sum_{j=1}^N \beta_{ij} \frac{p_i^{n+1} - p_i^n}{\tau} = -Ra \left( \sum_{i=1}^N (i\pi) \chi_{ij} d_i^{n+\frac{1}{2}} + \frac{\sqrt{2} \tanh \kappa_j}{\kappa_j} \right) [1 + \varepsilon \cos(n\omega\tau)] + \kappa_j^4 \frac{p_j^{n+1} + p_j^n}{2}, \quad (16a)$$

$$\tau_C \left[ \frac{d_j^{n+\frac{3}{2}} - 2d_j^{n+\frac{1}{2}} + d_j^{n-\frac{1}{2}}}{\tau^2} - \delta \sum_{i=1}^N b_{ij} \frac{p_i^{n+1} - p_i^n}{\tau} \right] + \frac{d_j^{n+\frac{3}{2}} - d_j^{n-\frac{1}{2}}}{2\tau} - \delta \sum_{i=1}^N b_{ij} \frac{p_i^{n+1} + p_i^n}{2} = -\frac{j^2 \pi^2 d_j^{n+\frac{3}{2}} + d_j^{n-\frac{1}{2}}}{Pr}. \quad (16b)$$

Here, we observe that Eq. (16b) also holds for the FHC case by simply setting  $\tau_C = 0$ . The stability and accuracy of this scheme (Eq. (16)) are discussed in [13], where it is shown that the convergence rate of the spectral coefficients  $p_i$ ,  $d_i$  is fifth-order algebraic for FHC; it is a straightforward task to extend those results to the MCHC case.

For the  $g$ -jitter case, the main effect is that the introduction of time varying gravity can bring about a parametric instability. This effect was first reported in [10], and later on thoroughly investigated by means of different numerical techniques in [11, 13], where extensive diagrams of the parametric instability were compiled. The amplitude  $\varepsilon$  of the oscillatory part of the gravitational acceleration plays the role of a bifurcation parameter. Depending on the physical parameters (i.e., the Rayleigh, Prandtl, and Cattaneo numbers), the threshold for  $\varepsilon$  varies, but the most important observation (first reported in [11]) is that for different frequencies, the oscillatory motion can be either isochronic, or a subharmonic bifurcation can take place. In this work we focus on cre-

ating the bifurcation diagram for the MCHC model and comparing it to the FHC-based results from [11, 13].

For the unsteady flow simulations, we again employ the parameter values  $Pr = 0.73$ ,  $Ra = 10^5$ ,  $\delta = 0.15$ , and  $\tau_C = 0.01$ . The results of these computations, generated using the scheme given in Eq. (16), are presented in Figure 2. For the overwhelming majority

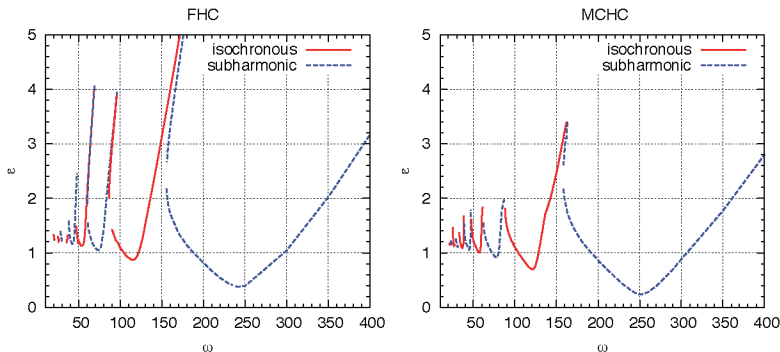


**FIGURE 2.** Bifurcation diagram for  $20 \leq \omega \leq 400$ . Left panel: FHC; Right panel: MCHC. In the left panel the branches in the  $\omega = 170$  region have been truncated for better comparison. They actually terminate at  $\varepsilon = 12.25$

of frequencies, we found that  $\varepsilon_{FHC} \geq \varepsilon_{MCHC}$ . This answers the question posed in the previous section regarding the comparative stability of the two models: Despite the appearance of a very damped non-oscillatory mode, the MCHC-based model loses stability in the  $g$ -jitter case earlier than the FHC-based one. We thus conclude that FHC is, in a sense, “more stable” than MCHC.

Another interesting observation is that some of the local minima in Figure 2 correspond to the imaginary parts of the eigenvalues in Table 1. For the MCHC case, we have  $\Im(\mu_3) = 252.49780$  and  $\Im(\mu_{17}) = 125.54751$  approaching the local minima at  $\omega = 252$  and  $\omega = 122$ . In the FHC case, the values  $\Im(\mu_1) = 76.68097$  and  $\Im(\mu_7) = 118.25278$  approach the local minima at  $\omega = 74$  and  $\omega = 116$  respectively. The imaginary parts of the eigenvalues found in the previous section are the oscillatory natural modes of the constant gravity system. The fact that the stability of the excited  $g$ -jitter system is reduced at  $\omega$  values that are close to those of the natural modes is a clear demonstration of resonance.

## CONCLUSIONS

We examined the effect of the Maxwell–Cattaneo law of heat conduction (MCHC) on two-gradient convection in a vertical slot. For the case of constant gravity, a truncated Galerkin expansion, based on Rayleigh’s beam functions for the stream function and trigonometric functions for the temperature, have been used. The eigenvalues of the resulting dynamical system show that for the parameter set considered, both the MCHC and Fourier conduction (FHC) cases are stable. However, the oscillatory modes of the MCHC model were found to decay slower than those of the FHC model.

For the case of gravity modulation, the expected pattern of alternating isochronous and subharmonic bifurcations was observed for both the FHC and MCHC models. The FHC-based solutions were found to be stable for larger values of the modulation amplitude than their MCHC counterparts. In addition, a correspondence between the minima in the stability diagrams and the imaginary parts of eigenvalues of the constant gravity flow was determined. This indicates that there is a resonant interaction between the modes of the constant gravity and  $g$ -jitter flows for both heat conduction models.

**Acknowledgment** The work of C.I.C. was supported, in part, by an ASEE/ONR Summer Faculty Fellowship.

## REFERENCES

1. P. M. Jordan, W. Dai, and R. E. Mickens, *Mech. Res. Commun.* **35**, 414–420 (2008).
2. D. D. Joseph and L. Preziosi, *Rev. Mod. Phys.* **61**, 41–73 (1989).
3. D. D. Joseph and L. Preziosi, *Rev. Mod. Phys.* **62**, 375–391 (1990).
4. D. S. Chandrasekharaiah, *Appl. Mech. Rev.* **51**, 705–729 (1998).
5. D. Jou, J. Casas-Vázquez, and G. Lebon, *Rep. Prog. Phys.* **62**, 1035–1142 (1998).
6. B. Straughan and F. Franchi, *Proc. Roy. Soc. Edinb.* **96A**, 175–178 (1984).
7. C. I. Christov and P. M. Jordan, *Phys. Rev. Lett.* **94**, 154301 (2005).
8. C. I. Christov, *Mech. Res. Comm.* **36**, 481–486 (2009).
9. J. W. Elder, *J. Fluid Mech.* **23**, 77–98 (1965).
10. A. Farooq and G. M. Homsy, *J. Fluid Mech.* **313**, 1–38 (1996).
11. C. I. Christov and G. M. Homsy, *J. Fluid Mech.* **430**, 335–360 (2001).
12. X. H. Tang and C. I. Christov, *Math. Comput. Simul.* **74**, 203–213 (2007).
13. N. C. Papanicolaou, C. I. Christov, and G. M. Homsy, *Int. J. Num. Meth. Fluids* **59**, 945–965 (2009).
14. C. I. Christov, “Frame Indifferent Form of Maxwell–Cattaneo Law,” in *Proceedings of the 8th International Congress on Thermal Stresses*, edited by M. Ostoja-Starzewski, and P. Marzocca, University of Illinois, 2009, vol. 2, pp. 543–546.
15. S. Chandrasekhar, *Hydrodynamic and Hydromagnetic Instability*, Oxford University Press, Clarendon, London, 1961.

## APPENDIX

### BEAM FUNCTIONS

Beam functions are the eigenfunctions of the fourth-order Sturm–Liouville BVP

$$u'''' = \lambda^4 u, \quad u' = 0, \quad \text{for } x = \pm 1. \quad (17)$$

The odd ( $s_m$ ) and even ( $c_m$ ) sets of eigenfunctions of (17) are

$$s_m = \frac{1}{\sqrt{2}} \left[ \frac{\sinh \lambda_m x}{\sinh \lambda_m} - \frac{\sin \lambda_m x}{\sin \lambda_m} \right], \quad c_m = \frac{1}{\sqrt{2}} \left[ \frac{\cosh \kappa_m x}{\cosh \kappa_m} - \frac{\cos \kappa_m x}{\cos \kappa_m} \right]. \quad (18)$$

The eigenvalues  $\lambda_m$  and  $\kappa_m$  are the solutions of

$$\coth \lambda_m - \cot \lambda_m = 0, \quad \tanh \kappa_m + \tan \kappa_m = 0. \quad (19)$$

Beam Function Expansion Formulas:

$$c'_n = \sum_{m=1}^{\infty} a_{nm} s_m, \quad s'_n = \sum_{m=1}^{\infty} \bar{a}_{nm} c_m, \quad a_{nm} = -\bar{a}_{mn} = \frac{4\kappa_n^2 \lambda_m^2}{\kappa_n^4 - \lambda_m^4}, \quad (20)$$

$$c''_n = \sum_{m=1}^{\infty} \beta_{nm} c_m, \quad \beta_{nm} = \begin{cases} \frac{4\kappa_n^2 \kappa_m^2}{\kappa_m^4 - \kappa_n^4} (\kappa_m \tanh \kappa_m - \kappa_n \tanh \kappa_n), & m \neq n, \\ \kappa_n \tanh \kappa_n - (\kappa_n \tanh \kappa_n)^2, & m = n, \end{cases} \quad (21)$$

$$s''_n = \sum_{m=1}^{\infty} \bar{\beta}_{nm} s_m, \quad \bar{\beta}_{nm} = \begin{cases} \frac{4\lambda_n^2 \lambda_m^2}{\lambda_n^4 - \lambda_m^4} (\lambda_n \coth \lambda_n - \lambda_m \coth \lambda_m), & m \neq n, \\ \lambda_n \coth \lambda_n - (\lambda_n \coth \lambda_n)^2, & m = n. \end{cases} \quad (22)$$

$$1 = \sum_{k=1}^{\infty} h_k c_k(x), \quad h_k = \int_{-1}^1 c_k(x) dx = \frac{2\sqrt{2} \tanh \kappa_k}{\kappa_k}. \quad (23)$$

$$\sin l\pi x = \sum_{k=1}^{\infty} \sigma_{lk} s_k(x), \quad \sigma_{lk} = \frac{2\sqrt{2} l \pi (\lambda_k)^2 (-1)^l}{l^4 \pi^4 - \lambda_k^4}, \quad (24a)$$

$$\cos l\pi x = \sum_{k=1}^{\infty} \chi_{lk} c_k(x), \quad \chi_{lk} = \frac{2\sqrt{2} \kappa_k^3 (-1)^{l+1} \tanh \kappa_k}{l^4 \pi^4 - \kappa_k^4}, \quad (24b)$$

$$c_n(x) = \sum_{l=1}^{\infty} \hat{\chi}_{nl} \cos l\pi x, \quad \hat{\chi}_{nl} = \frac{2\sqrt{2} \kappa_n^3 (-1)^{l+1} \tanh \kappa_n}{l^4 \pi^4 - \kappa_n^4}, \quad (24c)$$

$$s_n(x) = \sum_{l=1}^{\infty} \hat{\sigma}_{nl} \sin l\pi x, \quad \hat{\sigma}_{nl} = \frac{2\sqrt{2} l \pi (\lambda_n)^2 (-1)^l}{l^4 \pi^4 - \lambda_n^4}. \quad (24d)$$